COO-4927-09

DIRECT OBSERVATION OF ELECTRON TRANSFER ACROSS A LIPID BILAYER: LASER PHOTOLYSIS OF AN ASYMMETRIC VESICLE SYSTEM CONTAINING CHLOROPHYLL, METHYL VIOLOGEN, AND EDTA

William E. Ford and Gordon Tollin
Departments of Biochemistry and Chemistry
University of Arizona
Tucson, Arizona 85721

EHB

DISCLAIMER

Much previous experimentation has established that electron transfer across lipid bilayer vesicle walls can be photosensitized by amphiphilic dyes dissolved in the walls.[1-9] Membrane-bound electron carriers that shuttle electrons between the inner and outer bilayer-water interfaces are not required,[1,3-7,9] so it is usually presumed that electron transfer occurs by means of a direct interaction across the bilayer. We are examining such systems by laser flash photolysis to determine the mechanisms of charge transport across the membrane, so that the quantum yields of charge separation can be improved and devices that utilize vesicles to decompose water with sunlight can be realized. As will be described below, we have been able for the first time to directly observe all of the elementary processes involved in electron transfer across a bilayer. This provides us with a means of obtaining considerable insight into the factors that influence the efficiency of energy conversion in such systems.

The results and discussion presented here are restricted to vesicles whose walls contain phosphatidylcholine (from hens' egg yolks, abbreviated egg PC), chlorophyll a (Chl), and valinomycin; methyl viologen (MV^{2+}) is dissolved in the interior aqueous compartments of the vesicles as electron acceptor and ethylenediamine-N,N,N',N'-tetraacetate (EDTA) is dissolved in the continuous aqueous phase as electron donor. The aqueous phases are buffered at pH 8.4 with 0.9 M ammonium-potassium acetate. This system is analogous to one studied previously[6] except that we are using Chl instead of a tris-bipyridyl ruthenium complex as photosensitizer, and the locations of the viologen and EDTA are reversed. Valinomycin is added to facilitate cation transport through the vesicle wall.[9]

Laser photolysis was with red light (655-660 nm) excitation (10 ns pulse width). The instrumentation has been described previously[10]. The vesicle suspensions were deaerated with nitrogen.

Methyl viologen radical ($MV^{+\cdot}$) accumulates when the anaerobic vesicle suspensions are illuminated under steady-state conditions with orange light (>565 nm). Chl is catalytic in the process. The quantum yield of $MV^{+\cdot}$ production is of the order of 10^{-4}.

The triplet excited state of Chl (Chl^t) is quenched by MV^{2+} to produce $Chl^{+\cdot}$ and $MV^{+\cdot}$ (with subsequent radical recombination) in homogeneous and micellar media,[11,12] and this reaction occurs in the vesicle system as well. During the course of our laser photolysis experiments, it became clear that MV^{2+} dissolved in the internal aqueous volume of the vesicle suspension quenches only about 35% of the Chl^t (see below), which is reasonable if the interaction only occurs at the inner vesicle surface. Consequently, the absorbance changes due to photolysis contain contributions from unquenched Chl^t as well as from $Chl^{+\cdot}$ and $MV^{+\cdot}$ radicals. The reaction is best observed at 395 nm, where absorbance changes due to the radicals are positive and those due to the triplet are negative.[13,14]

We have examined vesicle suspensions (with varying Chl: egg PC mole ratios) that were prepared identically except that either MV^{2+} (0.10 M) or Na^+ (0.20 M) solutions were entrapped. The latter samples display laser-induced absorbance changes due to Chl^t alone, which could be subtracted from the composite transients to give difference signals ($\Delta(\Delta s)$) which are due just to the radicals. The baselines of the triplet and composite signals were adjusted relative to one another empirically to give satisfactory exponential fit to the decay of $\Delta(\Delta s)$. The absorbance changes at 395 nm up to 200 μs after the flash in the absence of EDTA, and with 0.40 M of EDTA, are reproduced in Fig. 1. It is clear that the rate of decay of the positive radical signal decreases and then increases as the Chl: egg PC mole ratio increases, and that the addition of EDTA increases the rate of radical decay. In the presence of EDTA, the composite signal becomes negative as the radical decays due to the negative contribution of unquenched Chl^t. At longer times after the laser flash

($\gtrsim$ 0.5 ms), the signal returns to the baseline with kinetics that parallel those of Chl^t decay.

Semilog plots representing radical decay at five EDTA concentrations, when the Chl: egg PC mole ratio is 1:450, are shown in Fig. 2. An exponential fit could be obtained in all cases examined. The dependence of the observed rate constant (k_{obs}) on EDTA concentration is shown in Fig. 3, when the Chl: egg PC mole ratios are 1:2800, 1:450, and 1:150. It is likely that the plots are sigmoidal in each case, with initial slopes that are small compared to the maximal ones.

The decay of the flash-induced absorbance increase at 465 nm, which is dominated by Chl^t during times less than 50 μs after the flash, is biphasic when MV^{2+} is entrapped, as compared to the decay when there is no MV^{2+} (Fig. 4). The initial concentration of Chl^t are nearly the same in both cases, indicating that there is little quenching of the excited singlet state of Chl by MV^{2+}. By moving the decay curve of unquenched Chl^t down, relative to the one containing both quenched and unquenched Chl^t, until the signal heights at about 50 μs are the same, we obtain the difference curve which is due to quenched Chl^t. The quenched Chl^t decays exponentially with a rate constant of 1.0×10^5 s^{-1}. From this we can calculate that the apparent bimolecular rate constant for quenching of Chl^t by entrapped MV^{2+} is 1.0×10^6 M^{-1} s^{-1}. This is similar to values obtained for quinone quenching of Chl^t in egg PC vesicles.[13] Based on the extrapolated signal heights at zero time attributable to quenched and unquenched Chl^t, we estimate that the fraction of total Chl^t that is quenched by MV^{2+} is 0.36. Using this fraction and the absorbance change due to Chl^+ and MV^+ radicals after the flash, the radical yield from quenched triplet is about 50% when the Chl: egg PC mole ratio is 1:450.

The reagents composing the vesicle system and the reactions between them are compartmentalized (see diagram).

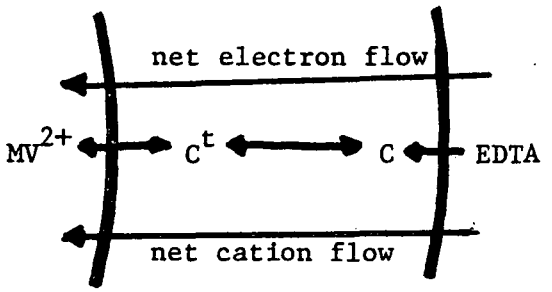

Chl is confined to the membrane phase, and MV^{2+} and EDTA are confined to the inner and outer aqueous phases, respectively. Only Chl in the inner monolayer of the vesicle wall reacts with MV^{2+}, producing $MV^{+\cdot}$ and $Chl^{+\cdot}$. $Chl^{+\cdot}$ disappears either by recombining with $MV^{+\cdot}$ or by reacting with EDTA. The first-order behavior of the recombination is similar to the $Chl^{+\cdot}$ - benzoquinone$^{-\cdot}$ recombination in vesicles.[13] The reaction with EDTA requires prior electron transport across the vesicle wall since $Chl^{+\cdot}$ is initially produced only at the inner water-bilayer interface and is inaccessible to the EDTA. Partioning of the disappearance of $Chl^{+\cdot}$ between these two paths depends on the relative rates of the radical recombination, transmembrane electron transport, and the reduction of $Chl^{+\cdot}$ (outside) by EDTA. We presume that electron transport through the bilayer is reversible.

Our experiments show that the rate of electron transfer across the vesicle wall can be $>10^4\ s^{-1}$, the approximate rate of recombination between $Chl^{+\cdot}$ and $MV^{+\cdot}$. This is the first such direct estimate of this rate. Our result is consistent with previous estimates of electron transport rates in analogous vesicle systems with a long-chained tris (2,2'-bipyridyl) ruthenium(II) photosensitizer instead of Chl[6]. Thus, as in that case, we can rule out "flip-flop" of the dye as the electron transport mechanism because flip-flop rates are slow by comparison ($\sim 10^{-7}$ to $10^0\ s^{-1}$, including Chl derivatives[15]). Therefore, of the two electron transport mechanisms previously considered,[6] via i) flip-flop or ii) electron-exchange between dye and oxidized dye that are in opposing monolayers, we favor the electron-exchange mechanism.

We find that k_{obs} in the absence of EDTA, when recombination between $MV^{+\cdot}$ and $Chl^{+\cdot}$ is the only decay pathway, decreases and then increases as the Chl: egg PC mole ratio increases. This result can be explained only if electron exchange processes are occurring. At low Chl: egg PC ratios, electron transfer across the bilayer is minimal and the recombination rate reflects mainly those processes occurring at the inner surface. As the ratio increases, the rate of recombination decreases due to rapid removal of $Chl^{+\cdot}$ from the site of primary electron transfer by exchange across the bilayer. The fact that at the highest Chl: egg PC ratio used here the rate constant becomes larger than it is at the lowest ratio implies that the rate of recombination at low Chl concentration is being controlled by diffusional processes occurring at the inner surface. By increasing the Chl concentration within the vesicle, a more facile recombination is permitted by virtue of a larger number of possible electron return routes resulting from Chl-to-$Chl^{+\cdot}$ electron exchanges occurring within the surface layer.

Saturation of k_{obs} with increasing EDTA concentration could be due to saturation of the vesicle surface with EDTA (i.e., the concentration of EDTA experienced by $Chl^{+\cdot}$ has a maximal value) or to complete capture of $Chl^{+\cdot}$ (outside) by EDTA.

The maximal slopes of the k_{obs} - versus-[EDTA] curves should increase with increasing Chl: egg PC mole ratio if electron transfer across the bilayer is via electron-exchange. Our data (Fig. 3) seem to bear out this prediction but lack sufficient resolution to be certain. This requires further investigation.

Thus we have developed a model vesicle system for studying photosensitized electron transfer across lipid bilayer membranes that is suitable for study by both kinetic and steady-state photochemical techniques. This system needs to be further examined before kinetic models can be developed and tested quantitatively so that the detailed mechanism of electron transfer across the membrane

can be determined. The ability to connect laser-photolytic and steady-state results is an important goal. The role that ion transport plays should be addressed. It should be possible to improve the quantum yields of charge separation by taking advantage of electrostatic potential gradients across the membrane-water interfaces[16] or across the membrane itself.[9] Eventually, this technology might be applied to the design of practial solar energy-converting devices that utilize pigmented vesicles.

This work is supported in part by a U.S. Department of Energy Research Contract.

References

1. Mangel, M., Biochim. Biophys. Acta 430, 459-466 (1976).
2. Ford, W. E., Otvos, J. W. & Calvin, M., Nature 274, 507-508 (1978).
3. Kurihara, K., Sukigara, M. & Toyoshima, Y., Biochim. Biophys. Acta 547, 117-126 (1979).
4. Kurihara, K., Toyoshima, Y. & Sukigara, M., Biochem. Biophys. Res. Commun. 88, 320-326 (1979).
5. Sudo, Y. & Toda, F., Nature 279, 807-809 (1979).
6. Ford, W. E., Otvos, J. W. & Calvin, M., Proc. Natl. Acad. Sci. USA 76, 3590-3593 (1979).
7. Sudo, Y. & Toda, F., J.C.S. Chem. Commun. 1979, 1044-1045.
8. Matsuo, T., Itoh, K., Takuma, K., Hashimoto, K. & Nagamura, T., Chem. Lett. 1980, 1009-1012.
9. Laane, C., Ford, W. E., Otvos, J. W. & Calvin, M., Proc. Natl. Acad. Sci. USA, in press.
10. Tollin, G., Castelli, F., Cheddar, G. & Rizzuto, F., Photochem. Photobiol. 29, 147-152 (1979).
11. Chibisov, A. K., Photochem. Photobiol. 10, 331-347 (1969).
12. Kiwi, J. & Grätzel, M., J. Phys. Chem. 84, 1503-1507 (1980).
13. Hurley, J. K., Castelli, F. & Tollin, G., Photochem. Photobiol. 32, 79-86 (1980).
14. Farrington, J. A., Ebert, M. & Land, E. J., J.C.S. Faraday Trans. I 1978, 665-675.
15. Birrell, G. B., Boyd, S. A., Keana, J. F. W. & Griffith, O. H., Biochim. Biophys. Acta 603, 213-219 (1980).
16. Turro, N. J., Grätzel, M. & Braun, A. M., Angew. Chem., Int. Ed. Engl. 19, 675-696 (1980).

FIGURE LEGENDS

Figure 1. Flash-induced absorbance changes at 395 nm in Chl-egg PC vesicle suspensions containing entrapped MV^{2+} aqueous solutions. The experiments in each column had the same Chl:egg PC mole ratio (1:2800, 1:450, or 1:150) and either no EDTA (first row) or 0.40 M of EDTA (second row) in the aqueous phase exterior to the vesicles. The abscissa is time after the laser flash (200 μs full scale).
Included are the decay curves of Chl^{t} in vesicles prepared without MV^{2+}. The vertical difference between the traces with MV^{2+} and those without MV^{2+} represents the absorbance change due to $Chl^{+}\cdot$ and $MV^{+}\cdot$ radicals (see text). Symmetric vesicle suspensions were prepared by injecting ethanol solutions of Chl and egg PC into vortex-stirred buffer (with or without 0.10M of MV^{2+}) followed by ultrasonication in a bath. The egg PC concentrations were either 3.5 mM (1:150 and 1:450 mole ratio samples) or 10.6 mM (1:2800 mole ratio sample). The vesicle suspensions were made asymmetric with respect to the aqueous phases by passing them through columns of Sephadex G-25 and SP-Sephadex C-25 that were pre-equilibrated with buffer (pH 8.4). EDTA was added as a 1.0 M solution of its ammonium salt.

Figure 2. First-order plots of the decay of the absorbance at 395 nm due to $Chl^{+}\cdot$ and $MV^{+}\cdot$ in vesicle suspensions with increasing concentrations of EDTA in the continuous aqueous phase. The Chl:egg PC mole ratio was 1:450.

Figure 3. Dependence of the first-order rate constants of the decay of absorbance at 395 nm due to $Chl^{+\cdot}$ and $MV^{+\cdot}$ in vesicle suspensions on exterior EDTA concentration. Chl:egg PC mole ratios were 1:2800 (O), 1:450 (Δ), or 1: 150 (■).

Figure 4. Flash-induced absorbance changes at 465 nm of Chl-egg PC vesicle suspensions without MV^{2+} (solid curve), and with 0.10 M MV^{2+} solution entrapped (broken curve).

1:2800 1:450 1:150

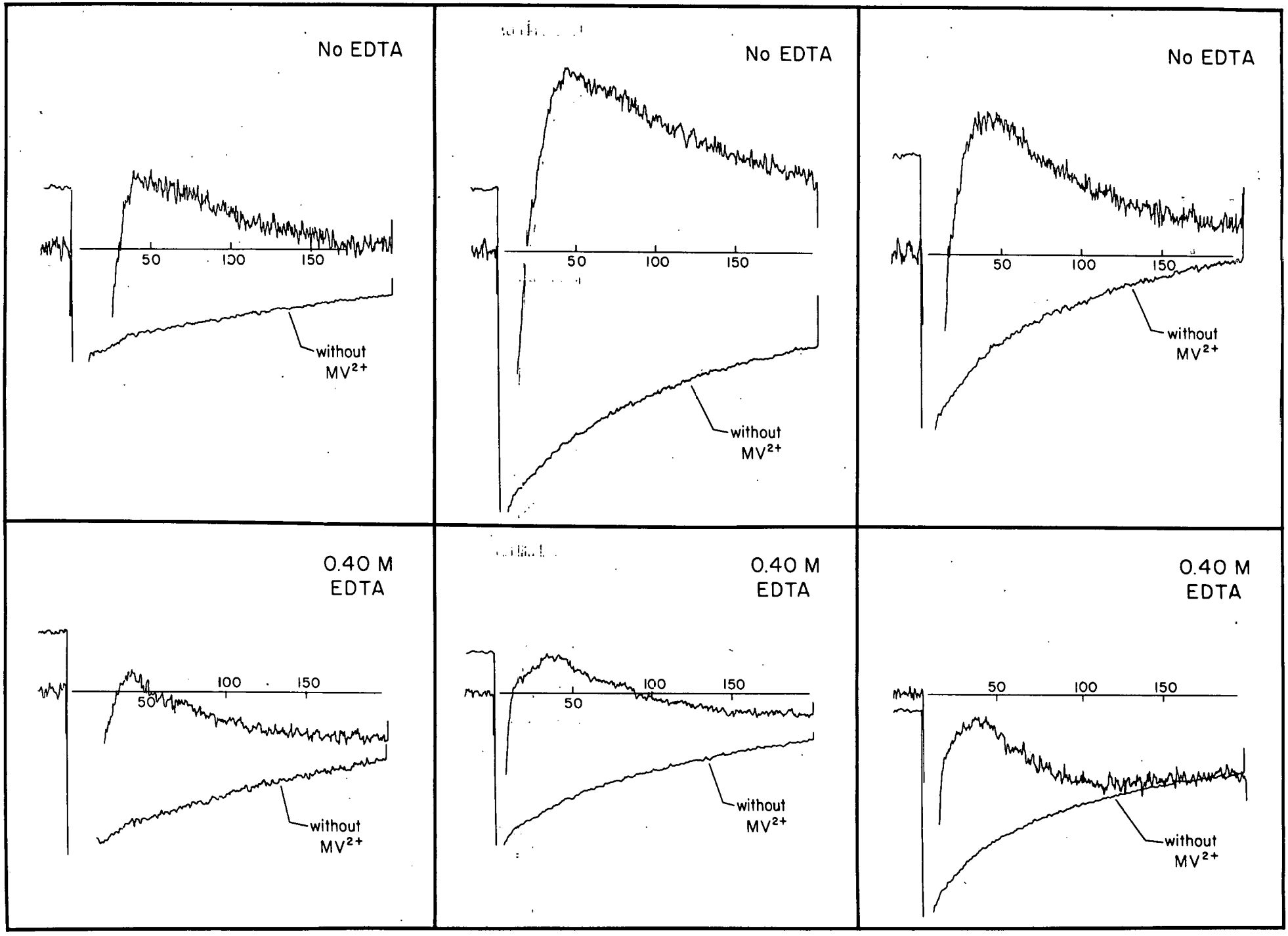

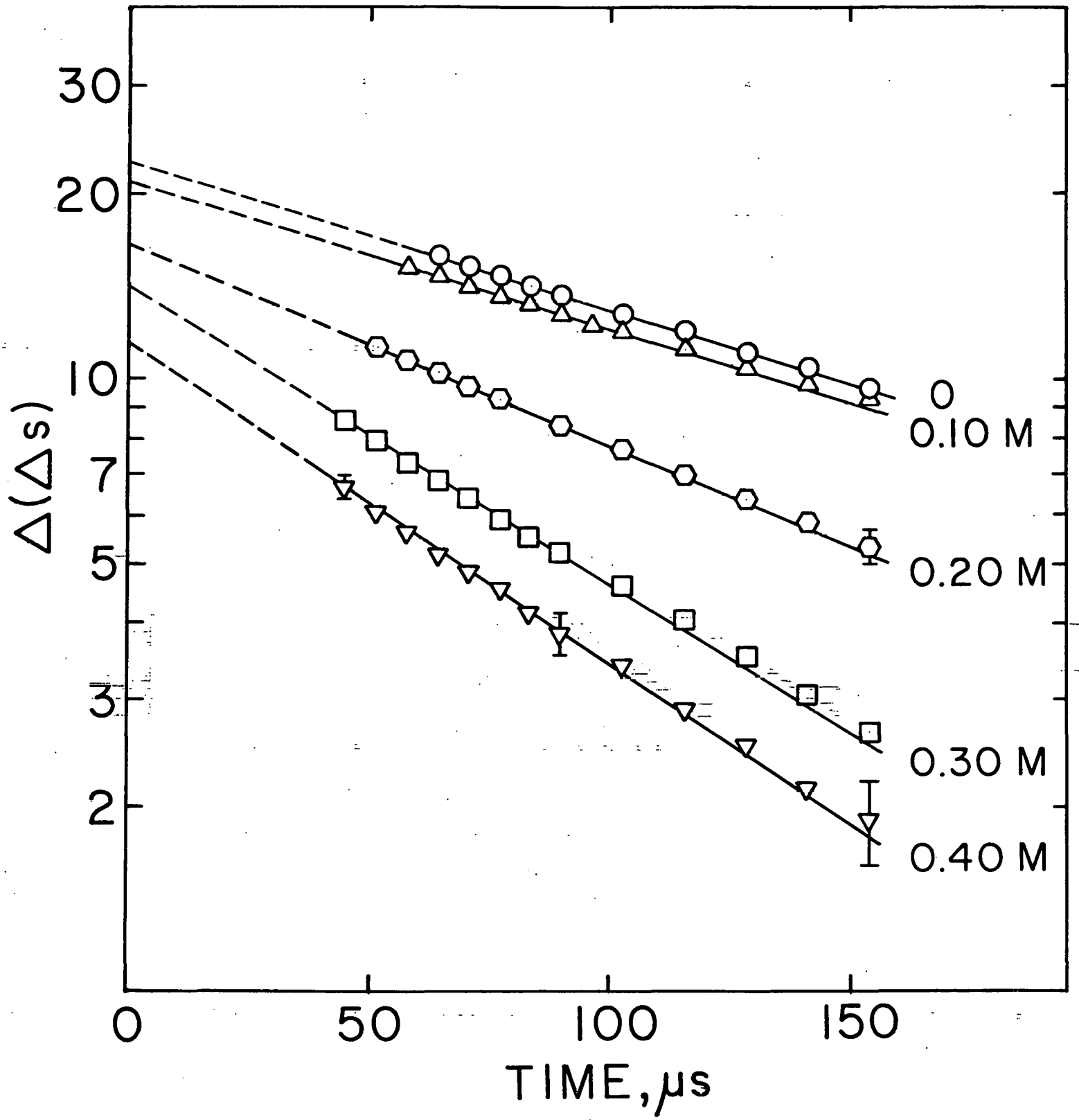
30
20
10
7
5
3
2
Δ(Δs)
0
0.10 M
0.20 M
0.30 M
0.40 M
0
50
100
150
TIME, μs

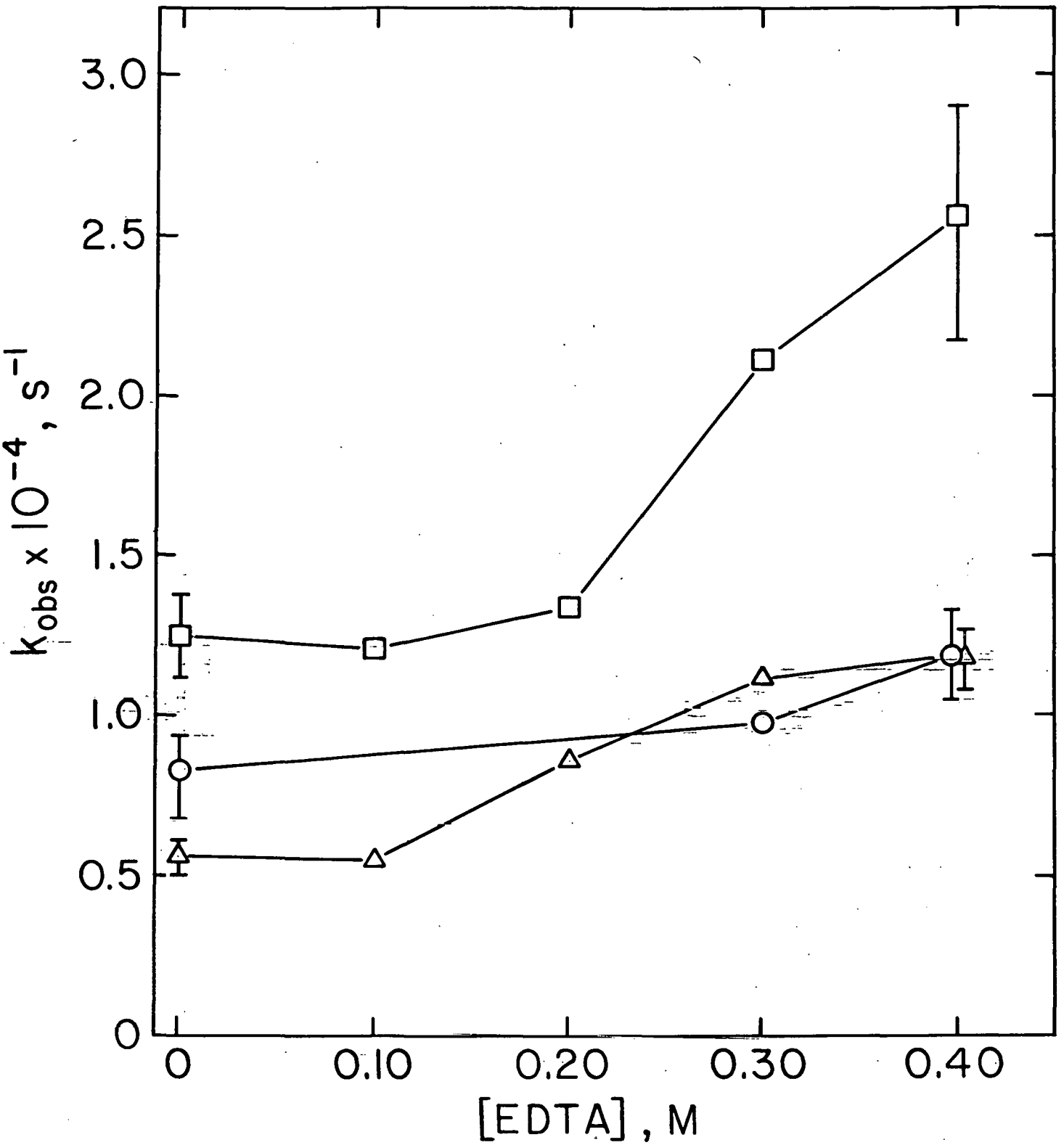
3.0
2.5
2.0
1.5
1.0
0.5
0
$k_{obs} \times 10^{-4}$, s^{-1}
0
0.10
0.20
0.30
0.40
[EDTA], M

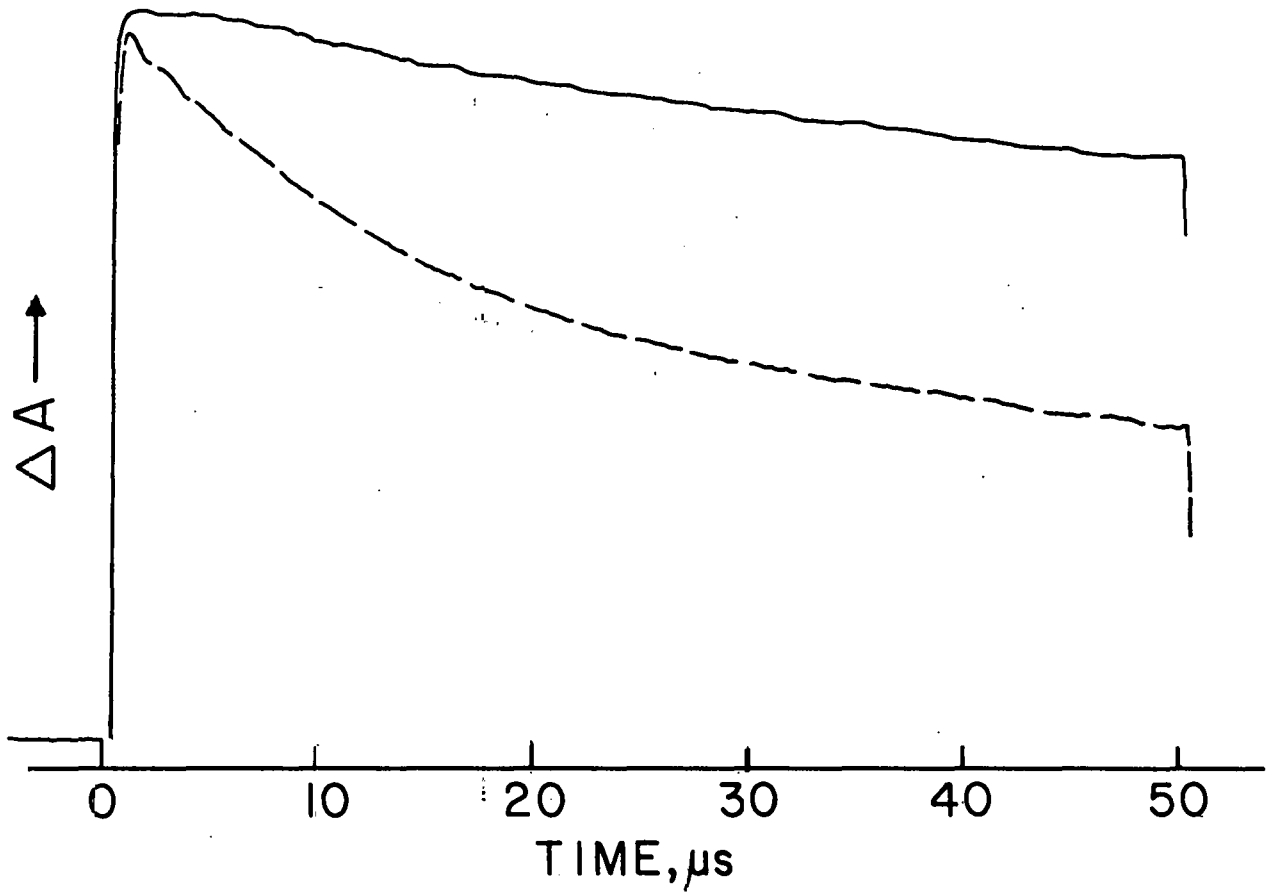
ΔA
0
10
20
30
40
50
TIME, μs